

See discussions, stats, and author profiles for this publication at: <https://www.researchgate.net/publication/231639803>

# Bonding Patterns in Benzene Triradicals from Structural, Spectroscopic, and Thermochemical Perspectives

ARTICLE *in* THE JOURNAL OF PHYSICAL CHEMISTRY A · JULY 2004

Impact Factor: 2.69 · DOI: 10.1021/jp049007j

---

CITATIONS

46

---

READS

18

3 AUTHORS, INCLUDING:



Yihan Shao

Q-Chem

69 PUBLICATIONS 3,165 CITATIONS

SEE PROFILE



Anna I Krylov

University of Southern California

178 PUBLICATIONS 6,999 CITATIONS

SEE PROFILE

# Bonding Patterns in Benzene Triradicals from Structural, Spectroscopic, and Thermochemical Perspectives

Ana-Maria C. Cristian,<sup>†</sup> Yihan Shao,<sup>‡</sup> and Anna I. Krylov<sup>\*,†</sup>

Department of Chemistry, University of Southern California, Los Angeles, California 90089-0482, and  
Q-Chem, Inc., The Design Center, Suite 690, 5001 Baum Blvd., Pittsburgh, Pennsylvania 15213

Received: March 4, 2004; In Final Form: May 13, 2004

Bonding patterns in tridehydrobenzenes are studied by electronic structure calculations. In all three isomers, the unpaired electrons form partial bonds between the radical centers. The strength of these bonds varies from a rather weak (but stabilizing) interaction of about 0.5 kcal/mol up to 32 kcal/mol, which is one-third of a typical chemical bond energy. The structural signature of these bonds is shorter distances between the radical centers relative to the closed-shell precursor. A doublet ground state is another manifestation of stabilizing interactions of unpaired electrons.

## I. Introduction

Highly reactive open-shell species play an important role in a variety of chemical processes. A large number of thermally activated and photochemical reactions have long been known to proceed through diradical intermediates.<sup>1,2</sup> More recently, polyradicals have become the focus of intense research due to their potential role as building blocks of organic magnets (see, for instance, refs 3–5).

Knowledge of factors that determine the electronic structure of polyradicals (e.g., ground state multiplicity, energy gaps between high-spin and low-spin states, etc.) is important for the design of magnetic materials as well as for an understanding of the reactivity of species with two or more unpaired electrons. Moreover, bonding patterns in systems with several unpaired electrons are of interest from a fundamental point of view. Indeed, in finite size species, the unpaired electrons are only nominally unpaired. In practice, their interactions can span the whole range from strongly antibonding (repulsion) to an almost complete chemical bond. These interactions have distinct structural, spectroscopic, and chemical signatures, and ultimately determine properties of open-shell compounds. For example, a bonding interaction between the unpaired electrons results in a shorter distance between the radical centers relative to a parent closed-shell molecule, and in more rigid structures, i.e., higher vibrational frequencies. The energetics of these partial bonds can be characterized by the so-called diradical and triradical stabilization energies (DSEs and TSEs), which provide a measure of the effect of combining two or more radical centers in the same molecule (which can be stabilizing or destabilizing with respect to the separate noninteracting centers). Finally, the ground-state multiplicity and the energy gap between the high-spin and low-spin states (e.g., the singlet–triplet and doublet–quartet splittings of the diradicals and triradicals, respectively) also represent a measure of the stabilizing or destabilizing interactions between the unpaired electrons. Indeed, a chemical bond is produced by a pair of electrons with antiparallel spins, while a system of noninteracting electrons would not show any preference for either high-spin or low-spin states.

From the electronic structure perspective, the type of interaction between the unpaired electrons is derived from the character of the MOs that host these electrons. In many di- and polyradicals, the nominally nonbonding MOs (NBMOs) interact either by direct spatial overlap (through-space interaction) or by overlap with intervening  $\sigma$  and  $\sigma^*$  orbitals (through-bond interaction<sup>6,7</sup>). The bonding interaction lifts the degeneracy between these orbitals, and when the MO splitting exceeds the electron repulsion, a pair of electrons occupies a bonding orbital (as dictated by the aufbau principle) thus producing a partial bond. However, when NBMOs are exactly degenerate, the aufbau principle, which is based on one-electron considerations only, predicts no energy difference between different electron arrangements. In this limiting case, the ground-state electronic configuration is determined by the electron repulsion that is minimal for the same spin electrons. Thus, for degenerate NBMOs the extension of Hund's first rule<sup>8</sup> to molecules predicts that the lowest energy state is the one with the highest multiplicity, i.e., triplet, quartet, quintet, etc. However, violations of this rule occur when the singly occupied NBMOs are disjoint,<sup>9–11</sup> i.e., localized on different parts of the molecule. In this case, the exchange interactions between these orbitals are small, and low-spin and high-spin states with the same spatial configuration are nearly degenerate. In some cases, mixing with certain singly excited configurations can lower the energy of the low-spin state, but not that of the high-spin state, and the former falls below the latter. This mechanism of reversing the singlet–triplet ordering has been termed dynamic spin polarization.<sup>12,13</sup> Although these guiding rules—the aufbau principle and extended Hund's rule—have proved to be extremely useful in predicting the ground-state multiplicity, it is often unclear which one would prevail. Indeed, there is no quantitative criterion of separating the aufbau and Hund's domains, and the decisive word belongs to either an experiment or predictive electronic structure calculations.

This work analyzes the bonding in the tridehydrobenzene isomers (1,2,3-, 1,2,4-, and 1,3,5- $C_6H_3$ ) according to the criteria mentioned above. We report equilibrium structures, doublet–quartet energy gaps, and TSEs. The electronic structure of several low-lying excited states is also discussed.

The structure of the paper is as follows. Section II describes methodological issues relevant to triradicals and outlines the

\* Address correspondence to this author.

<sup>†</sup> University of Southern California.

<sup>‡</sup> Q-Chem, Inc.

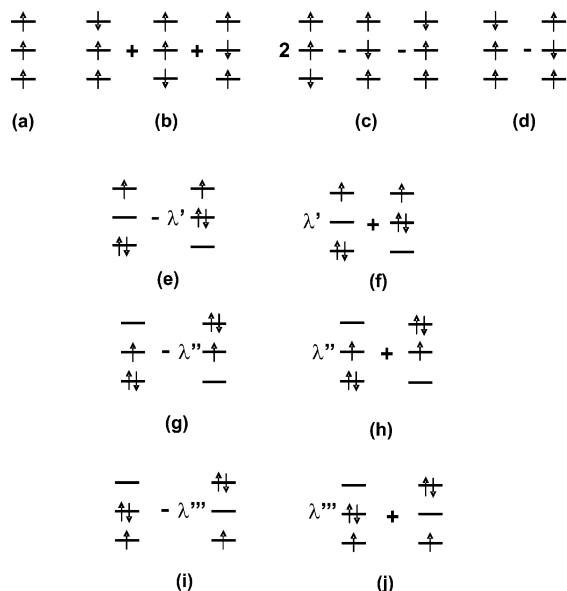


**Figure 1.** Wave functions of triradicals that are eigenfunctions of  $\hat{S}^2$ . Note that all the  $M_S = 1/2$  configurations present in the low-lying triradical states [wave functions b–j] are formally obtained from the  $M_S = 3/2$  reference state (a) by single excitations including a spin-flip. The coefficients  $\lambda$  that define the mixing of closed-shell determinants depend on the energy spacing between the orbitals, while the coefficients of the open-shell determinants are determined solely by the spin symmetry requirements. Spatial symmetry determines further mixing of the above wave functions.

SF approach. In Section III, the results are presented: the analysis of the  $C_6H_3$  low-lying states (III.A), their structures (III.B), and thermochemistry (III.C). Our concluding remarks are given in Section IV.

## II. Theoretical Methods

**A. Triradicals and the Spin-Flip Approach.** Triradicals—species with three unpaired electrons distributed over three nearly degenerate orbitals—feature extensive electronic degeneracies that result in multiconfigurational wave functions.<sup>14</sup> The complexity of the triradical electronic structure and, consequently, the challenges they pose for electronic structure methodology exceed even those of diradicals.<sup>13,15–17</sup> Figure 1 shows valid triradical wave functions with a positive projection of the total spin, i.e., with  $M_S = +3/2, 1/2$ . Note that only the high-spin component of the quartet state, configuration (a) in Figure 1, is single-configurational, while all the low-spin states are multiconfigurational and are, therefore, not accessible by the traditional ground-state single-reference methods. However, all these states can accurately be described by the spin-flip (SF) models.<sup>18–23</sup> In the SF approach, low-spin states are described as spin-flipping excitations from a high-spin reference state, for which effects due to dynamical and nondynamical correlation are much smaller than those for the corresponding low-spin states.<sup>18</sup>

In the case of triradicals, the SF method describes target states as

$$\Psi_{M_S=1/2}^{d,q} = \hat{R}_{M_S=-1} \tilde{\Psi}_{M_S=3/2}^q \quad (1)$$

where  $\tilde{\Psi}_{M_S=3/2}^q$  is the  $\alpha\alpha\alpha$  high-spin reference determinant [configuration a in Figure 1],  $\hat{R}_{M_S=-1}$  is an excitation operator that flips the spin of an electron ( $\alpha \rightarrow \beta$ ), and  $\Psi_{M_S=1/2}^{d,q}$  stands for the wave functions of the doublet and quartet target states

b–j. Since all the configurations (with  $M_S = 1/2$ ) present in the low-lying triradical states [wave functions b–j in Figure 1] are formally obtained from the  $M_S = 3/2$  reference state by single excitations including a spin-flip, the SF method provides a balanced description of all the triradical states from Figure 1.

Note that, although all the target states (the quartet b, the open-shell doublets c and d, and the closed-shell doublets e–j) are multiconfigurational, they are treated by SF within a single-reference formalism.

As in traditional (non-SF) models, the description of the target states can be improved systematically by employing increasingly accurate models for the reference state. Recent benchmarks<sup>17</sup> demonstrated that the accuracy of the SF methods is roughly the same as that of the corresponding non-SF models in the case of well-behaved closed-shell systems. The SF approach thus extends traditional methods to diradicals, triradicals, and bond breaking. Other advantages of the SF methods are their multistate nature (several excited states, for example, all the triradical states in Figure 1, can be obtained in a single calculation) and the fact that they do not require the selection of an active space.

Three SF models are employed in this study: two models based on the equation-of-motion coupled-cluster (EOM-CC) formalism,<sup>24,25</sup> and the SF extension of time-dependent density-functional theory (TDDFT).<sup>26–29</sup> In the EOM-SF-CCSD<sup>23</sup> and EOM-SF-OD<sup>18</sup> models, the reference state is described by coupled-cluster singles-and-doubles (CCSD)<sup>24</sup> and optimized-orbitals coupled-cluster doubles (OO-CCD or simply OD),<sup>24,30,31</sup> respectively. In these models, the operator  $\hat{R}$  includes single and double excitations which flip the spin of an electron. EOM-SF-CCSD and EOM-SF-OD have been shown to yield accurate excitation energies and singlet–triplet gaps for diradicals:<sup>17,23</sup> typical and maximum errors were about 1 and 3 kcal/mol, respectively. Here, we employed these models to calculate doublet–quartet gaps. Most of the equilibrium geometries were calculated by the SF-DFT method<sup>21</sup> with the 50/50 functional.<sup>32</sup> SF-DFT has been found to yield accurate equilibrium geometries for diradicals and triradicals,<sup>14,17,21,33</sup> the typical error in bond lengths being less than 0.01 Å. The performance of SF-DFT in calculating equilibrium properties is thus superior to that of multiconfigurational self-consistent field (MCSCF), which yields bond distances with typical errors of 0.06 Å.

**B. Accurate Thermochemistry of Open-Shell Species: High-Spin Pathways for Calculating Diradical and Triradical Stabilization Energies.** A measure of the strength of the interaction between one radical center and a diradical moiety is provided by the triradical stabilization energy (TSE).<sup>34</sup> For the trihydrobenzene isomers, TSE is defined as the energy at 0 K ( $\Delta E_0^0$ ) of hypothetical isodesmic reactions (see Figure 2) in which a radical center is transferred from a triradical to a benzene molecule, yielding a phenyl radical and a benzyne diradical as products. A positive value of the TSE indicates stabilization of the triradical relative to separated radical centers. This definition of TSE is analogous to that given by Wierschke et al.<sup>35</sup> for the diradical stabilization energy (DSE) of the benzyne isomers. In their paper, DSE is calculated as the energy change in the reaction between a benzyne molecule and benzene, in which two phenyl radicals are formed; this is also the approach we employ in this work for the calculation of the DSEs of benzyne. Experimentally, TSEs and DSEs can be determined from heats of formation.<sup>34,36,37</sup>

While there is only one way to separate the two radical centers in a diradical, there are, in general, several possible channels for the separation of a radical center from a triradical. For

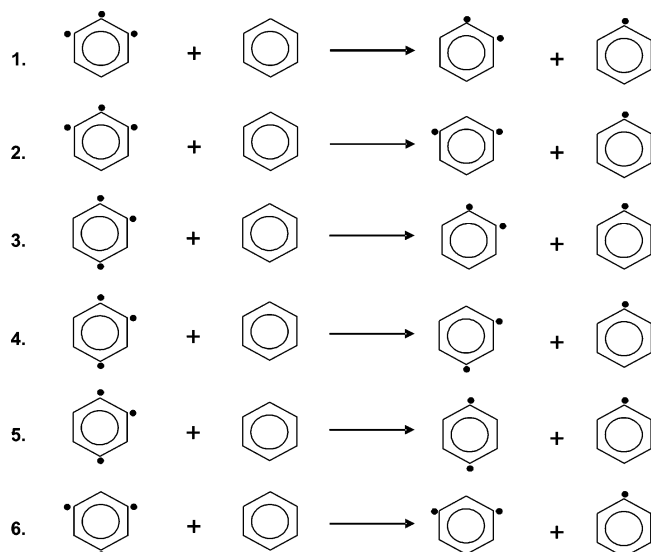


**Figure 2.** Isodesmic reactions whose energy changes define the triradical stabilization energies for the  $C_6H_3$  isomers. Contrary to diradicals, in triradicals there are in general several ways to separate the third radical center from a diradical moiety.

example, in the case of 1,2,3- and 1,2,4- $C_6H_3$ , the reaction with benzene may proceed on two and three different channels, respectively. As can easily be proved, however, for a given triradical the sum of TSE and the DSE of the benzyne product is the same for all the TSE channels—simply because there is only one way to separate all three radical centers. Therefore, if a TSE for a triradical can be accurately determined (theoretically or experimentally), the other TSEs of the same triradical may be calculated indirectly, using the DSEs of the corresponding diradicals. For example, the experimental TSEs for reactions 2, 4, and 5 given in Table 3 were not determined directly, but were calculated by using TSEs for reactions 1 and 3, provided in refs 34 and 36, and the DSEs of benzyne calculated from experimental heats of formation given in the Appendix.

Theoretical calculations of TSEs and DSEs are rather challenging due to the fact that the species involved in the corresponding reactions have very different electronic structure (i.e., some of them are well-behaved closed-shell molecules that can be described by single-reference methods, while others are open-shells with multiconfigurational wave functions), which makes it virtually impossible to find a method that will describe all of them with a similar accuracy. For instance, the ground (low-spin) states of the triradicals and diradicals involved in the isodesmic reactions 1–6 are multiconfigurational (see the discussion in section III.A for the  $C_6H_3$  isomers and that in ref 17 for benzyne). On the other hand, the ground states of benzene and phenyl are dominated by a single configuration. This is why it is not possible to calculate TSE in a balanced way by either a single-reference or a multireference method. However, the high-spin components of the lowest quartet and triplet states of the  $C_6H_3$  and  $C_6H_4$  isomers, respectively, are single-determinantal, which makes possible the accurate computation of high-spin TSEs (i.e., the energy change in the reactions shown in Figure 2 where the triradicals and diradicals are in their lowest quartet and triplet states, respectively) by a suitable single-reference model.

This is the essence of our approach to the calculation of TSEs and DSEs, which is illustrated in Figure 3. The low-spin TSE is calculated from the high-spin TSE [determined at the CCSD(T)/cc-pVTZ level] and the doublet–quartet ( $\Delta E_{DQ}$ ) and singlet–triplet ( $\Delta E_{ST}$ ) gaps of the triradical and diradical species,

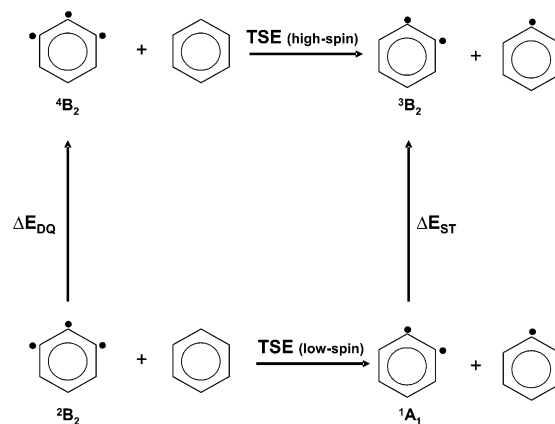


**Figure 3.** Determination of the triradical stabilization energy (TSE) by high-spin pathways, exemplified by the case of 1,2,3-tridehydrobenzene. The low-spin TSE (the reaction energy of the low-spin reaction) is calculated from the corresponding high-spin TSE and the doublet–quartet and singlet–triplet gaps of the triradical and diradical, respectively.

respectively. Accurate values of  $\Delta E_{DQ}$  and  $\Delta E_{ST}$  can be calculated by a SF or multireference method or else taken from experiment.<sup>38</sup> In this work, the SF-CCSD and SF-OD models were employed.

This approach is expected to lead to efficient error cancellation. Although only a triple- $\zeta$  basis is used, one may expect an accuracy of  $\sim 1$  kcal/mol for the high-spin reactions, due to their isodesmic character.<sup>39</sup> The errors in TSE are thus dominated by those in  $\Delta E_{DQ}$  and  $\Delta E_{ST}$ . While very detailed benchmarks are necessary to determine error bars for SF, previous results for diradicals<sup>17</sup> indicate a typical error of  $\sim 1$  kcal/mol in the singlet–triplet gaps. Moreover, it was found that for diradicals with a singlet ground state, SF methods systematically underestimate  $\Delta E_{ST}$ ,<sup>17</sup> so that we expect error cancellation in the calculation of any low-spin TSE, in whose expression  $\Delta E_{DQ}$  for a triradical with a doublet ground state and  $\Delta E_{ST}$  for a diradical with a singlet ground state appear with opposite signs.

To minimize errors in the computed energies that are due to the spin contamination of the radical species, the simplest approach is to use a restricted open-shell (ROHF) reference in the CC calculations.<sup>40</sup> The resulting correlated wave function is not spin pure, since in its spin–orbital formulation the cluster operator  $\hat{T}$  does not commute with the total spin operator  $\hat{S}^2$ . It can easily be shown, however, that the spin contaminants in the ROHF-CC wave function do not contribute directly to the energy,<sup>40,41</sup> although they do contribute indirectly, through the wave function optimization.<sup>41</sup> Additional calculations were performed by using the Brueckner CCD model<sup>42</sup> in which orbitals are optimized for the correlated CCD wave function.

**C. Computational Details.** The equilibrium structures of the lowest quartet states of the tridehydrobenzenes ( $^4B_2$  in 1,2,3- and 1,3,5- $C_6H_3$  and  $^4A'$  in 1,2,4- $C_6H_3$ ) and of the lowest triplet states of the benzyne ( $^3B_2$  in *o*- and *m*-benzyne and  $^3B_{1u}$  in *p*-benzyne) were calculated by density-functional theory with a B3LYP<sup>43</sup> functional, and the CCSD method with perturbative account of the triples, CCSD(T).<sup>43</sup> The 6-311G\*\*<sup>46,47</sup> and cc-pVTZ<sup>48</sup> basis sets, respectively, were employed. Pure angular momentum functions (5d, 7f) were used throughout this study.

The ground states of the tridehydrobenzenes ( $^2B_2$ ,  $^2A'$ , and  $^2A_1$  in 1,2,3-, 1,2,4-, and 1,3,5- $C_6H_3$ , respectively), as well as the ground states of the benzyne ( $^1A_1$  in *o*- and *m*-benzyne, and  $^1A_{1g}$  in *p*-benzyne) were optimized by using the SF-DFT method<sup>21</sup> with a 50/50 functional<sup>32</sup> and a 6-311G\*\* basis set.



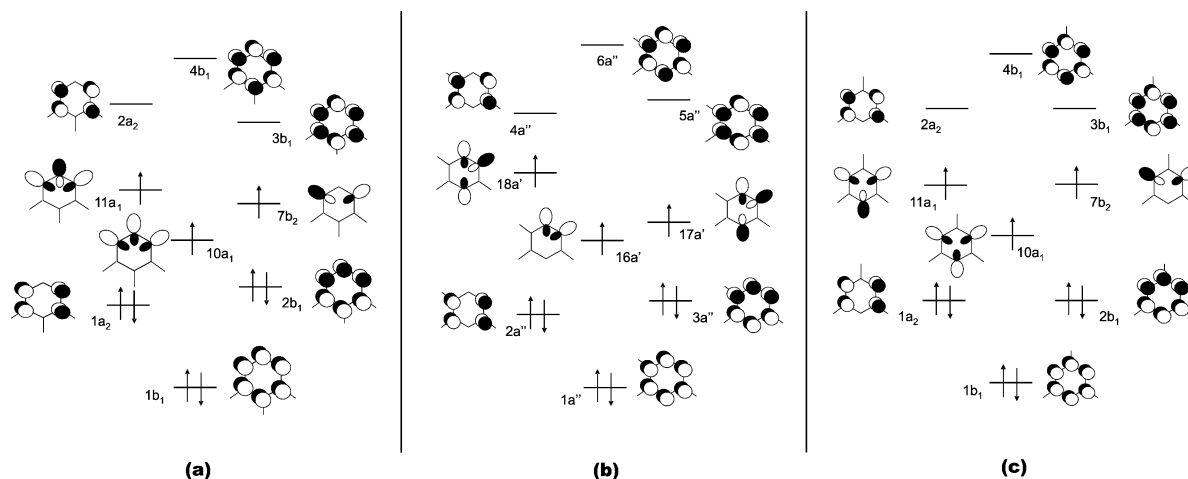


**Figure 4.** Molecular orbitals of (a) 1,2,3- $\text{C}_6\text{H}_3$ , (b) 1,2,4- $\text{C}_6\text{H}_3$ , and (c) 1,3,5- $\text{C}_6\text{H}_3$ . Only the  $\pi$ -system, which is similar to that in benzene, and the three  $\sigma$  orbitals, which in the lowest quartet state host unpaired electrons, are shown.

The geometry of the  $\tilde{X}^2\text{A}_1$  ground state of the phenyl radical was optimized at the B3LYP/6-311G\*\* level. For the ground state of benzene, the CCSD(T)/cc-pVQZ equilibrium structure from ref 49 was used.

Doublet–quartet and singlet–triplet adiabatic energy separations for all the triradicals and diradicals were calculated at the SF-DFT/6-311G\*\* level, and also by the EOM-SF-CCSD<sup>23</sup> method with a mixed basis set (cc-pVTZ on carbon and cc-pVDZ<sup>48</sup> on hydrogen). Both unrestricted and restricted open-shell Hartree–Fock references were employed in the EOM-SF-CCSD calculations.

The high-spin TSEs for the isodesmic reactions 1–6 (see Figure 2) were computed at the CCSD(T)/cc-pVTZ level. Additional calculations of the high-spin TSEs were performed by using Brueckner CCD with perturbative triples, BCCD(T).<sup>50</sup>

Zero-point vibrational energies were calculated by density-functional theory (B3LYP/6-311G\*\*) for the high-spin states of the triradicals and diradicals and also for the ground states of benzene and phenyl. ZPEs of the ground (low-spin) states of the  $\text{C}_6\text{H}_3$  and  $\text{C}_6\text{H}_4$  isomers were determined by using the SF-DFT method and a 6-311G\*\* basis set.

All the SF and DFT calculations were performed by using the Q-CHEM<sup>51</sup> ab initio package. The CCSD(T) results were obtained with the ACES II<sup>52</sup> electronic structure package. Some basis sets were obtained from the EMSL database.<sup>53</sup>

### III. Results and Discussion

**A. Low-Lying Electronic States in  $\text{C}_6\text{H}_3$  Isomers: Molecular Orbital Picture.** Molecular orbitals of the  $\text{C}_6\text{H}_3$  isomers are shown in Figure 4. The three  $\sigma$  orbitals derived from the three  $\text{sp}^2$ -hybridized orbitals of the dehydrocarbons are between the bonding and antibonding  $\pi$ -orbitals. The  $\pi$ -system of the trihydrobenzenes is similar to that of benzene.

In trihydrobenzenes, three electrons are distributed in the three nearly degenerate  $\sigma$  orbitals. This can be done in several ways (see Figure 1). If these orbitals were all exactly degenerate, the ground state of the molecule would be a quartet, according to Hund's rule. If the orbitals are well-separated in energy, however, the aufbau principle would predict a doublet ground state, in which the lowest triradical orbital is doubly occupied and the singly occupied orbital is the second lowest.

For the  $\text{C}_6\text{H}_3$  isomers, the aufbau principle prevails over Hund's rule and their ground states are closed-shell-type doublets, the corresponding wave function being denoted by configuration g in Figure 1. The ground state dominant con-

figuration, in all three cases, has the lowest triradical orbital ( $10a_1$  in **1** and **3**, and  $16a'$  in **2**) doubly occupied and the next orbital ( $7b_2$ ,  $17a'$ , and  $11a_1$  in **1**, **2**, and **3**, respectively) singly occupied. The closed-shell doublet ground state of these triradicals is a signature of a bonding interaction between the unpaired electrons. The doublet–quartet gaps are presented and discussed in section III.C.

In 1,2,3- $\text{C}_6\text{H}_3$ , the  $\tilde{X}^2\text{B}_2$  ground state is followed in energy by the  $1^2\text{A}_1$  state, whose wave function is of type e: the dominant configuration has the  $10a_1$  orbital doubly and the  $11a_1$  orbital singly occupied. The next state is the  $1^4\text{B}_2$  quartet, whose  $M_S = 3/2$  and  $1/2$  components are shown in Figure 1, configurations a and b, respectively. The  $M_S = 3/2$  component of this state was used as the spin-flip reference. Higher in energy there are two doublet states,  $1^2\text{B}_1$  and  $1^2\text{A}_2$ , derived from the excitation of an electron from the  $1a_2$  and  $2b_1$   $\pi$  orbitals to the  $10a_1$   $\sigma$  orbital.

In the 1,2,4-isomer, the triradical orbitals are all of the same symmetry ( $a'$ ), and the low-lying triradical states shown in Figure 1 that are of the same multiplicity can mix. The  $\tilde{X}^2\text{A}'$  ground state is a closed-shell doublet of type g. The next in energy is the  $2^2\text{A}'$  state, which is predominantly of type i, but also has contributions from configurations in which all the triradical orbitals are singly occupied. The second excited state is the lowest quartet,  $1^4\text{A}'$ , whose  $M_S = 3/2$  component was chosen as the spin-flip reference for 1,2,4- $\text{C}_6\text{H}_3$ . Two states of  $\text{A}''$  symmetry that are derived from  $\pi \rightarrow \sigma$  excitations lie higher in energy. The dominant configuration in the lowest  $\text{A}''$  state has the  $3a''$ ,  $17a'$ , and  $18a'$  orbitals singly occupied and  $16a'$  doubly occupied, while in the next state the configuration that results from a  $2a'' \rightarrow 16a'$  excitation of the reference state is dominant. However, for both states, the configurations resulting from the excitation of an electron from the other occupied  $\pi$  orbitals ( $1a''$ ,  $3a''$  and  $1a''$ ,  $2a''$ , respectively) have rather large coefficients (at the ground state and lowest quartet geometries).

In 1,3,5- $\text{C}_6\text{H}_3$ , the  $\tilde{X}^2\text{A}_1$  ground state is a closed-shell-type doublet [g in Figure 1, where the orbitals are  $10a_1$ ,  $11a_1$ , and  $7b_2$  in the order of increasing energy]. Next in energy are the  $1^2\text{B}_2$  state, whose wave function is of type e, and the lowest quartet,  $1^4\text{B}_2$ .

Similarly to the other isomers, the third and fourth excited states ( $1^4\text{A}_2$  and  $1^4\text{B}_1$ ) are derived from the excitation of one electron from a  $\pi$  orbital ( $2b_1$  and  $1a_2$ , respectively) into the lowest triradical ( $\sigma$ ) orbital ( $10a_1$ ). These two states are

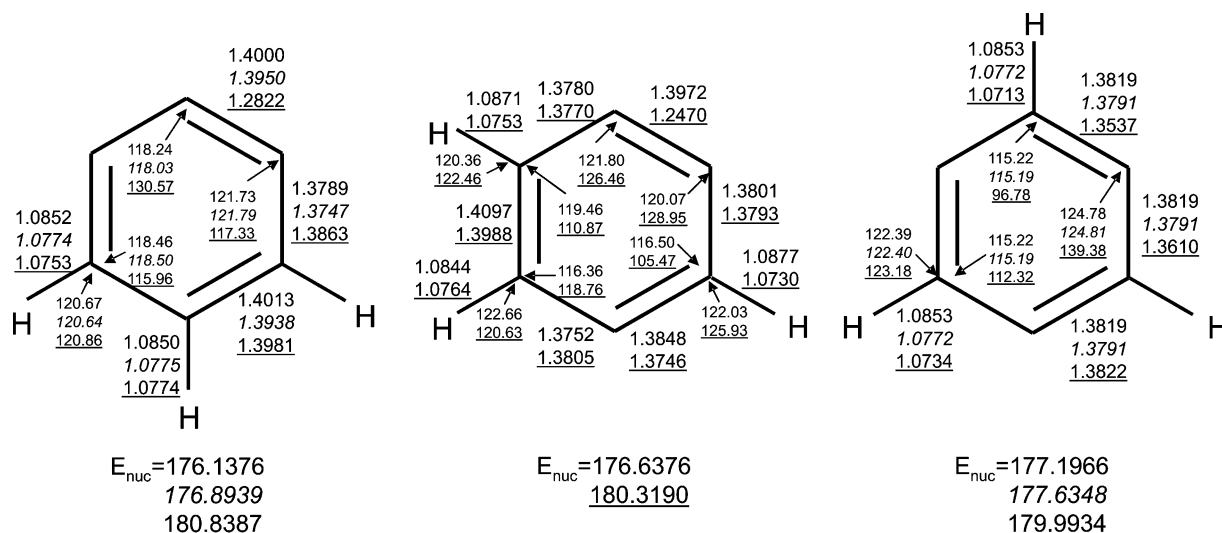


**Figure 5.** Equilibrium structures of 1,2,3-, 1,2,4-, and 1,3,5- $\text{C}_6\text{H}_3$  (1, 2 and 3). The lowest high-spin (quartet) states have been optimized at the B3LYP/6-311G\*\* and CCSD(T)/cc-pVTZ levels. The ground (doublet) state parameters have been calculated at the SF-DFT/6-311G\*\* level. Bond lengths are in angstroms, angles in degrees, and nuclear repulsion energies in hartrees.

degenerate in  $D_{3h}$  symmetry (e.g., at the equilibrium geometry of the  $1^4\text{B}_2$  state).

A thorough discussion of these states of the 1,3,5-isomer, as well as of higher electronically excited states, is given in ref 14.

**B. Equilibrium Structures.** Equilibrium structures of the ground and lowest quartet states of 1, 2, and 3 are shown in Figure 5. For the quartet states of 1 and 3, the B3LYP/6-311G\*\* structures are very similar to the CCSD(T)/cc-pVTZ ones and were used in subsequent calculations.

The bonding character of the lowest  $\sigma$  molecular orbital (see Figure 4) suggests a bonding interaction between the unpaired electrons, resulting in shorter distances between the radical centers than in benzene. Indeed, the calculated equilibrium structures manifest considerably contracted distances that demonstrate partial bond formation between the radical centers. The magnitude of the distance decrease is related to the strength of these partial bonds. Figure 6 shows the relative changes in the distances between trihydrocarbons (in the  $\text{C}_6\text{H}_3$  isomers) and dihydrocarbons (in the  $\text{C}_6\text{H}_4$  species) with respect to the corresponding distances in the benzene molecule. The changes are calculated as  $\Delta r/r_{\text{benz}}$ , where  $\Delta r$  is the deviation of the distance between radical centers in a given triradical or diradical from the distance between carbon atoms situated in the same positions in benzene (denoted by  $r_{\text{benz}}$ ). These values quantify the effect of the interaction between radical centers on the structures of the di- and trihydrobenzenes.

In the  $\tilde{X}^2\text{B}_2$  ground state of 1,2,3- $\text{C}_6\text{H}_3$ , the shortening of the distance between meta radical centers is much less pronounced than that in the  $\tilde{X}^1\text{A}_1$  state of *m*-benzyne, while the bond between ortho dehydrocarbons is only slightly longer than the one in the  $\tilde{X}^1\text{A}_1$  state of *o*-benzyne. This implies that in the ground state of 1, the ortho interaction prevails over the meta one, but is weaker than that in *o*-benzyne, due to  $\sigma$  delocalization over dehydrocarbons C1, C2, and C3.

In 1,2,4- $\text{C}_6\text{H}_3$  ( $\tilde{X}^2\text{A}'$  state), the C1–C2 bond is almost as short as the one in *o*-benzyne, while the distance between the meta radical centers at C2 and C4 is considerably longer than that in *m*-benzyne, but shorter than that in 1,2,3- $\text{C}_6\text{H}_3$ . This suggests that, although the interaction between the ortho radical centers at C1 and C2 prevails, the interaction between the C2 and C4 dehydrocarbons also has a noticeable effect on the structure of 2. The fact that the distance between the para

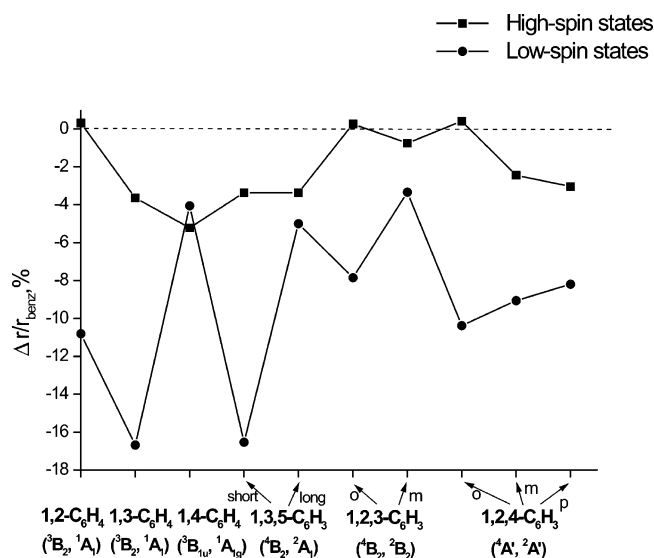


**Figure 6.** Relative change of the distance between radical centers in benzenes ( $\text{C}_6\text{H}_4$ ) and trihydrobenzenes ( $\text{C}_6\text{H}_3$ ) with respect to benzene. For each species,  $\Delta r/r_{\text{benz}}$  (in %) for the ground (low-spin) state and for the lowest high-spin state is shown. For the  $\text{C}_6\text{H}_3$  isomers, all possible distances between two radical centers are considered; for example, in 1,2,4- $\text{C}_6\text{H}_3$ , the distances between centers in ortho (o), meta (m), and para (p) positions are used.

dehydrocarbons C1 and C4 is shorter than in *p*-benzyne is probably due to an overall tighter structure rather than a stronger interaction between these radical centers.

In 1,3,5- $\text{C}_6\text{H}_3$ , whose  $\tilde{X}^2\text{A}_1$  ground state is a Jahn–Teller distorted doublet,<sup>14</sup> the distance between the C1 and C3 dehydrocarbons is much shorter than the C1–C5 and C3–C5 distances between the other radical centers in the meta position. The C1–C3 distance is only slightly longer than the one in *m*-benzyne, so it can be concluded that the radical center at C5 interacts very weakly with the diradical moiety in 3.<sup>14,34</sup>

Even in the high-spin states of the  $\text{C}_6\text{H}_3$  and  $\text{C}_6\text{H}_4$  isomers, the distances between meta and para radical centers are contracted relative to benzene. This has been explained to be a consequence of an increase in electron density in the central part of these molecules upon C–H bond breaking.<sup>14</sup> For radical centers in the ortho position, this effect is compensated by the

**TABLE 1: Singlet–Triplet and Doublet–Quartet Energy Separations (eV) for Di- and Tridehydrobenzenes<sup>a</sup>**

	1,2-C <sub>6</sub> H <sub>4</sub>	1,3-C <sub>6</sub> H <sub>4</sub>	1,4-C <sub>6</sub> H <sub>4</sub>	1,2,3-C <sub>6</sub> H <sub>3</sub>	1,2,4-C <sub>6</sub> H <sub>3</sub>	1,3,5-C <sub>6</sub> H <sub>3</sub>
SF-DFT/6-311G**	1.896	0.986	0.179	2.489	2.084	1.515
SF-CCSD(UHF)/mixed <sup>b</sup>	1.629	0.834	0.171	2.235	1.863	1.197
SF-CCSD(ROHF)/mixed <sup>b</sup>	1.626	0.805	0.171	2.137	1.786	1.198
SF-OD/mixed <sup>b,c</sup>	1.632	0.837	0.171			
experiment <sup>d</sup>	1.628 ± 0.013	0.911 ± 0.014	0.165 ± 0.016			

<sup>a</sup> ZPEs not included. <sup>b</sup> cc-pVTZ basis on carbon and cc-pVDZ on hydrogen. <sup>c</sup> Data from ref 17. <sup>d</sup> Data from ref 38.

**TABLE 2: Reaction Energies at 0 K (kcal/mol) for the High-Spin<sup>a</sup> Idodesmic Reactions 1 to 6<sup>b</sup> (high-spin TSEs)**

method/basis set <sup>c</sup>	1	2	3	4	5	6
UHF-CCSD(T)/cc-pVTZ	−9.04	−10.47	−2.77	−4.20	−7.91	−4.33
ROHF-CCSD(T)/cc-pVTZ	−9.05	−13.03	−2.97	−6.95	−8.12	−6.15
BCCD(T)/cc-pVTZ	−9.28	−13.11	−3.18	−7.01	−8.31	−6.52
ΔZPE <sup>d</sup>	−0.40	−0.52	−0.30	−0.42	−0.37	−0.16

<sup>a</sup> The lowest triplet states of the diradicals and the lowest quartet states of the triradicals are involved in the reactions. <sup>b</sup> See Figure 2. <sup>c</sup> For benzene, the RHF-CCSD(T)/cc-pVTZ energy was employed in all cases. <sup>d</sup> Zero-point vibrational energies calculated at the B3LYP/6-311G\*\* level.

**TABLE 3: Reaction Energies at 0 K (kcal/mol) for the Low-Spin<sup>a</sup> Idodesmic Reactions 1 to 6<sup>b</sup> (low-spin TSEs)**

TSE	1	2	3	4	5	6
theory <sup>c</sup>	2.35	17.17	0.43	15.25	28.75	2.75
experiment <sup>d</sup>	12.3 ± 4.9	28.3 ± 6.7	4.0 ± 5.8	20.0 ± 7.4	35.9 ± 7.3	3.7 ± 5.6

<sup>a</sup> The ground states (singlet and doublet, respectively) of the diradicals and triradicals are involved in the reactions. <sup>b</sup> See Figure 2. <sup>c</sup> Low-spin TSEs calculated with use of SF-CCSD (ROHF) gaps for the triradicals and diradicals and ROHF-based CCSD(T)/cc-pVTZ high-spin TSEs. <sup>d</sup> TSEs for reactions 1, 3, and 6 from refs 34 and 36. TSEs for reactions 2, 4, and 5 calculated as explained in Section II B.

strong electron repulsion, and the distance between C1–C2 dehydrocarbons is slightly elongated with respect to benzene.

To summarize, the equilibrium structures of the C<sub>6</sub>H<sub>3</sub> and C<sub>6</sub>H<sub>4</sub> isomers indicate the formation of partial bonds between the radical centers in these species.

**C. Doublet–Quartet Gaps, Thermochemistry, and Tri-radical Stabilization Energies.** As explained in section II B, tri-radical stabilization energies (TSEs) for the ground (low-spin) states of the C<sub>6</sub>H<sub>3</sub> isomers were calculated by using high-spin TSEs and the doublet–quartet and singlet–triplet gaps for tridehydrobenzenes and benzyne, respectively.

The extent of the interaction between the “unpaired” electrons in the ground (low-spin) state and in the lowest high-spin state is reflected in the value of the adiabatic energy separation between these states. Thus, in benzyne, as the distance between radical centers increases (from ortho to meta to para), the energy of the low-spin state becomes higher (as the bonding interaction becomes weaker), while the high-spin state is lowered in energy, due to weaker electron repulsion. This results in a decrease of the singlet–triplet gap as ortho > meta > para. In tridehydrobenzenes, the strongest bonding interaction in the low-spin state and the strongest repulsion in the high-spin state both occur in the 1,2,3-isomer, where the three radical centers are closest together, resulting in the largest doublet–quartet gap. The relative stability of the ground and lowest quartet states of the 1,2,4- and 1,3,5-isomers is less obvious a priori. From the EOM-SF-CCSD calculations, we found that the bonding interaction in the  $\tilde{X}^2A'$  state of **2** is stronger than that in the  $\tilde{X}^2A_1$  state of **3**, while the lowest high-spin states of the two molecules are very close in energy. This results in a larger doublet–quartet gap in the 1,2,4-isomer. In conclusion, the most efficient bonding interaction occurs in the ground state of the 1,2,3-isomer, followed by the 1,2,4- and 1,3,5-isomers, respectively.

Caution should be exercised when performing calculations for open-shell species, even for relatively well-behaved high-spin states. In particular, the quality of the results can be affected by spin-contamination. Although the highly correlated CC models are relatively insensitive to the orbital choice, and the

**TABLE 4: Diradical Stabilization Energies (DSEs) for Benzyne (kcal/mol)**

	<i>o</i> -C <sub>6</sub> H <sub>4</sub>	<i>m</i> -C <sub>6</sub> H <sub>4</sub>	<i>p</i> -C <sub>6</sub> H <sub>4</sub>
theory <sup>a</sup>	30.89	16.66	1.30
theory + experiment <sup>b</sup>	31.82	17.63	2.09
experiment <sup>c</sup>	35.4 ± 3.3	19.4 ± 3.2	3.5 ± 3.0

<sup>a</sup> High-spin DSEs calculated by CCSD(T)/cc-pVTZ (with a ROHF reference). Singlet–triplet gaps, computed by SF-OD with a mixed basis set (cc-pVTZ on C, cc-pVDZ on H), are from ref 17. <sup>b</sup> ROHF-CCSD(T)/cc-pVTZ high-spin DSEs and experimental singlet–triplet gaps<sup>38</sup> were used. <sup>c</sup> Experimental DSEs calculated from heats of formation given in the Appendix.

corresponding wave functions exhibit only very small residual spin-contamination,<sup>41,54</sup> its effect on the CCSD(T) or EOM-CCSD energies can be significant.<sup>55</sup> Therefore, we performed CC calculations using UHF, ROHF, and Brueckner orbitals. High-spin TSEs, calculated at the CCSD(T)/cc-pVTZ level with UHF and ROHF references, are given in Table 2. BCCD(T) TSEs for all reactions are also shown in Table 2. For reactions 2, 4, and 6, differences larger than 2 kcal/mol between the UHF- and ROHF-based high-spin TSEs are observed. As expected, Brueckner calculations support the ROHF-based results.

The highest exothermicity is manifested in reactions 1 and 2, in which one radical center is separated from the other two in 1,2,3-C<sub>6</sub>H<sub>3</sub>. This is not surprising, since the repulsion between the unpaired electrons in the lowest quartet state is strongest in the 1,2,3-isomer. A large negative value of  $\Delta E_0^o$  is also obtained for reaction 5, in which the radical center at dehydrocarbon C2, whose repulsive interaction with radical centers in ortho and meta positions is strong, is separated from the triradical.

Low-spin TSEs and DSEs are given in Tables 3 and 4, respectively, and illustrated in Figure 7. By comparing the TSE values for different reactions, several conclusions regarding the extent of the interaction between radical centers can be drawn. First, as expected, in a given triradical the strength of the interaction decreases as the distance between the radical centers increases (from ortho to meta to para).

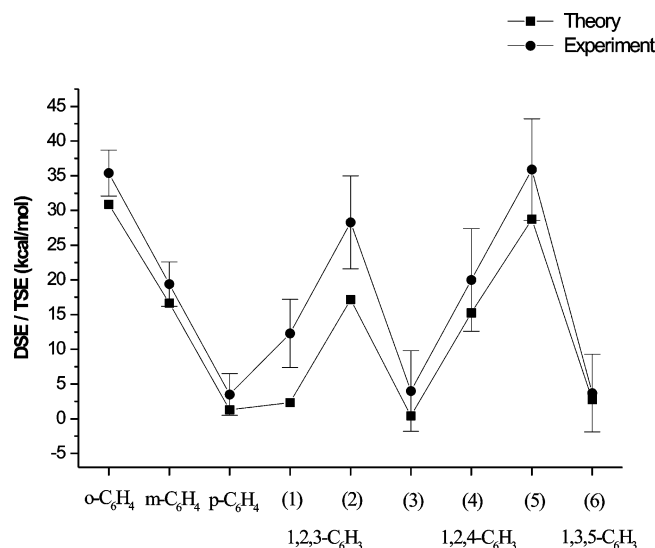


**Figure 7.** Theoretical and experimental values of DSEs and TSEs for benzynes and trihydrobenzenes (obtained as explained in Tables 3 and 4). Labels (1)–(6) correspond to the isodesmic reactions in Figure 2.

In 1,2,3- $\text{C}_6\text{H}_3$ , the interaction between centers situated in an ortho position is much stronger than the meta interaction, as proved by the small TSE of reaction 1. In 1,2,4- $\text{C}_6\text{H}_3$ , the ortho interaction is also dominant (the TSE of reaction 3 is very small). For 1,3,5- $\text{C}_6\text{H}_3$ , it can be concluded from the small TSE of reaction 6 that the third radical center interacts very weakly with the *m*-benzyne moiety.

As follows from Tables 3 and 4, and Figure 7, the overall trend in theoretical TSEs and DSEs closely follows the experimental one. However, some theoretical values fall outside of the experimental error bars, which deserves further analysis.

The best theoretical estimates for DSEs are within the experimental error bars for *m*- and *p*-benzyne; however, DSE for *o*-benzyne is 1.2 kcal/mol lower than the lowest experimental estimate. To check different error sources, we recalculated DSEs by using experimental singlet–triplet gaps.<sup>38</sup> The overall changes are small (within 1 kcal/mol), and the *o*-benzyne's DSE is now only 0.28 below the lowest experimental estimate. Taking into account estimated error bars of 1 kcal/mol for the theoretical value, this value agrees with the experimental one.

Calculation of the high-spin DSE for *o*-benzyne by BCCD-(T)/cc-pVTZ yields a result that differs by only 0.12 kcal/mol from the ROHF-CCSD(T)/cc-pVTZ one. Since *o*-benzyne is the most well-behaved of all isomers, and can accurately be described by single-reference methods, we recalculated the low-spin DSE by the CCSD(T) and B-CCD(T) methods (with the cc-pVTZ basis). The corresponding values are 30.80 and 30.61 kcal/mol, respectively, both being in excellent agreement with the theoretical DSE from Table 4. This further supports the theoretical DSE.

Figure 8 presents a comparison of our best estimate of *o*-benzyne's DSE (calculated by using the experimental singlet–triplet gap, as explained above) with experimental DSEs, obtained from the heats of formation of *o*-benzyne given in ref 38, Table 3. Taking into consideration the experimental and theoretical error bars, our value is in good agreement with four of the eight measurements, and very close to other two. As described above, it is in agreement with the recommended weighted average value (no. 9 in Figure 8). We also calculated the weighted average of the experimental data excluding experiments 3 and 4 that considerably differ from those of

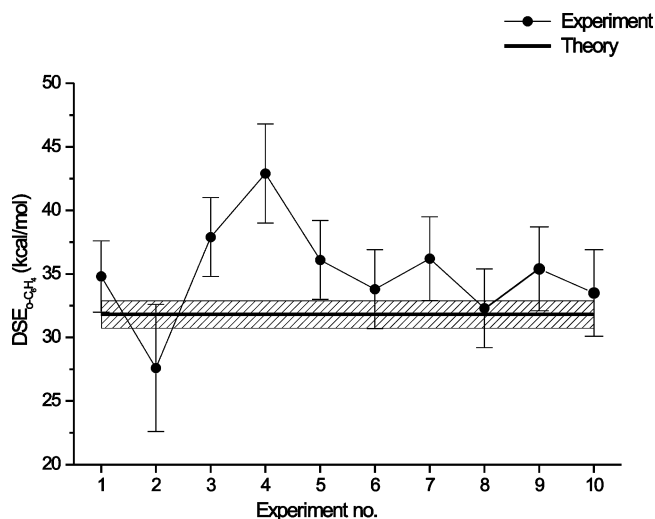


**Figure 8.** A comparison of the best theoretical estimate of *o*-benzyne's DSE with the available experimental values. The theoretical value is obtained by using the experimental singlet–triplet gap, as explained in Table 4. The hatched area illustrates the estimated uncertainty ( $\pm 1$  kcal/mol) in the theoretical DSE. The experimental DSEs were calculated with use of the thermochemical data from Table 5 and the heats of formation of *o*-benzyne provided in Table 3 of ref 38. The numbering of the experiments follows the ordering therein. The last two values are weighted averages of the experiments 1–8 and 1,2,5–8, respectively.

experiments 1, 2, and 5–8. The resulting value of  $33.5 \pm 3.4$  kcal/mol (no. 10 in Figure 8) is even in better agreement with the theoretical value. Overall, the agreement of the theoretical DSE with the experimental values is good, while the large discrepancies between different experiments suggest that the recommended experimental value should be refined.

The calculated TSEs for 1,2,4- and 1,3,5- $\text{C}_6\text{H}_3$  are in good agreement with experiment. However, for 1,2,3- $\text{C}_6\text{H}_3$ , both theoretical TSEs are 4–5 kcal/mol lower than the lowest experimental value. The most conservative estimate of error bars for calculated TSEs is considerably smaller than 4 kcal/mol—thus, the experimental and computational error bars do not overlap. To further clarify this point, the TSE corresponding to reaction 1 was calculated at the CCSD(T)/cc-pVTZ level with an ROHF reference. Since the ground states of both 1,2,3- $\text{C}_6\text{H}_3$  and *o*-benzyne at their equilibrium geometries are dominated by a single configuration, the TSE thus computed can be considered accurate within 1 kcal/mol. This value is larger than the TSE calculated following the high-spin pathway by only 0.45 kcal/mol, which argues in favor of the accuracy of the theoretical TSE for this reaction. The discrepancy between the theoretical and experimental results may be due to the error in the reference thermochemical data employed to calculate the heat of formation of 1,2,3- $\text{C}_6\text{H}_3$  from the experimentally measurable data.

#### IV. Conclusions

The electronic structure of the trihydrobenzene triradicals is characterized by coupled-cluster methods. We find that in all three isomers, the bonding character of the lowest NBMO is sufficiently strong for the aufbau principle to win over Hund's rule. The resulting doublet ground states exhibit partial bond formation between the radical centers. In agreement with a qualitative MO analysis, the doublet–quartet gaps and, therefore, the strength of the bonding interactions decrease in the following sequence: 1,2,3 > 1,2,4 > 1,3,5. The energy of these partial bonds is characterized by TSE and DSE. In benzynes, the



**TABLE 5: Supplemental Thermochemical Data**

compd	$\Delta H^\circ_{f,298}(\text{g})$ , kcal/mol	ref
<i>o</i> -C <sub>6</sub> H <sub>4</sub>	105.9 ± 3.3	<i>a</i>
<i>m</i> -C <sub>6</sub> H <sub>4</sub>	121.9 ± 3.1	<i>b</i>
<i>p</i> -C <sub>6</sub> H <sub>4</sub>	137.8 ± 2.9	<i>b</i>
C <sub>6</sub> H <sub>6</sub>	19.7 ± 0.3	<i>b</i>
C <sub>6</sub> H <sub>5</sub>	80.5 ± 0.5	<i>c</i>

<sup>a</sup> Reference 38. <sup>b</sup> Reference 57. <sup>c</sup> Reference 58.

stabilizing interaction between the radical centers varies from 4 to 32 kcal/mol, the latter value being close to a third of a normal chemical bond energy. In tridehydrobenzenes, the interaction between the third center and the diradical moiety varies in a similar range (0.4–30 kcal/mol). The calculated TSEs are in reasonable agreement with experiment and the detailed analysis is in favor of the theoretical TSEs.

**Acknowledgment.** Support from the National Science Foundation CAREER Award (grant no. CHE-0094116), the Alfred P. Sloan foundation, the WISE Research Fund (USC), and the donors of the Petroleum Research Fund, administered by the American Chemical Society (PRF-AC), is gratefully acknowledged. We thank Prof. Paul G. Wenthold for stimulating discussions and sharing his results prior to publication.

## Appendix

The heats of formation used to calculate experimental DSEs from Table 4 and TSEs for reactions 2, 4, and 5 from Table 3 are provided in Table 5.

## References and Notes

- (1) Turro, N. *Modern Molecular Photochemistry*; Benjamin/Cummings Publishing Co.: Menlo Park, CA, 1978.
- (2) Platz, M. S., Ed. *Kinetics and spectroscopy of carbenes and biradicals*; Plenum Press: New York, 1990.
- (3) Rajca, A. *Chem. Rev.* **1994**, *94*, 871.
- (4) Iwamura, H. *J. Phys. Org. Chem.* **1998**, *11*, 299.
- (5) Crayston, J. A.; Devine, J. N.; Walton, J. C. *Tetrahedron* **2001**, *56*, 7829.
- (6) Hoffmann, R. *Acc. Chem. Res.* **1971**, *4*, 1.
- (7) Crawford, T. D.; Kraka, E.; Stanton, J. F.; Cremer, D. *J. Chem. Phys.* **2001**, *114*, 10638.
- (8) For a thorough discussion of Hund's rules and their domain of validity, see: Kutzelnigg, W.; Morgan, J. D., III *Z. Phys. D* **1996**, *36*, 197.
- (9) Borden, W. T.; Davidson, E. R. *J. Am. Chem. Soc.* **1977**, *99*, 4587.
- (10) Borden, W. T.; Iwamura, H.; Berson, J. A. *Acc. Chem. Res.* **1994**, *27*, 109.
- (11) Hrovat, D. A.; Borden, W. T. *J. Mol. Struct. (THEOCHEM)* **1997**, *398–399*, 211.
- (12) Kollmar, H.; Staemmler, V. *Theor. Chim. Acta* **1978**, *48*, 223.
- (13) Borden, W. T., Ed. *Diradicals*; Wiley: New York, 1982.
- (14) Slipchenko, L. V.; Krylov, A. I. *J. Chem. Phys.* **2003**, *118*, 9614.
- (15) Salem, L.; Rowland, C. *Angew. Chem., Int. Ed. Engl.* **1972**, *11*, 92.
- (16) Bonačić-Koutecký, V.; Koutecký, J.; Michl, J. *Angew. Chem., Int. Ed. Engl.* **1987**, *26*, 170.
- (17) Slipchenko, L. V.; Krylov, A. I. *J. Chem. Phys.* **2002**, *117*, 4694.
- (18) Krylov, A. I. *Chem. Phys. Lett.* **2001**, *338*, 375.
- (19) Krylov, A. I. *Chem. Phys. Lett.* **2001**, *350*, 522.
- (20) Krylov, A. I.; Sherrill, C. D. *J. Chem. Phys.* **2002**, *116*, 3194.
- (21) Shao, Y.; Head-Gordon, M.; Krylov, A. I. *J. Chem. Phys.* **2003**, *118*, 4807.
- (22) Sears, J. S.; Sherrill, C. D.; Krylov, A. I. *J. Chem. Phys.* **2003**, *118*, 9084.
- (23) Levchenko, S. V.; Krylov, A. I. *J. Chem. Phys.* **2004**, *120*, 175.

- (24) Purvis, G. D.; Bartlett, R. J. *J. Chem. Phys.* **1982**, *76*, 1910.
- (25) Stanton, J. F.; Bartlett, R. J. *J. Chem. Phys.* **1993**, *98*, 7029.
- (26) Runge, E.; Gross, E. K. U. *Phys. Rev. Lett.* **1984**, *52*, 997.
- (27) Petersilka, M.; Grossman, U. J.; Gross, E. K. U. *Phys. Rev. Lett.* **1996**, *76*, 1212.
- (28) Bauernschmitt, R.; Ahlrichs, R. *Chem. Phys. Lett.* **1996**, *256*, 454.
- (29) Hirata, S.; Head-Gordon, M. *Chem. Phys. Lett.* **1999**, *314*, 291.
- (30) Scuseria, G. E.; Schaefer, H. F. *Chem. Phys. Lett.* **1987**, *142*, 354.
- (31) Sherrill, C. D.; Krylov, A. I.; Byrd, E. F. C.; Head-Gordon, M. J. *Chem. Phys.* **1998**, *109*, 4171.
- (32) 50% Hartree–Fock + 8% Slater + 42% Becke for exchange and 19% VWN + 81% LYP for correlation.
- (33) Slipchenko, L. V.; Krylov, A. I. *J. Chem. Phys.* **2003**, *118*, 6874.
- (34) Lardin, H. A.; Nash, J. J.; Wenthold, P. G. *J. Am. Chem. Soc.* **2002**, *124*, 12612.
- (35) Wierschke, S. G.; Nash, J. J.; Squires, R. R. *J. Am. Chem. Soc.* **1993**, *115*, 11958.
- (36) Lardin, H. A.; Wenthold, P. G. Manuscript in preparation.
- (37) Slipchenko, L. V.; Munsch, T. E.; Wenthold, P. G.; Krylov, A. I. *Angew. Chem., Int. Ed.* **2003**, *43*, 742.
- (38) Wenthold, P. G.; Squires, R. R.; Lineberger, W. C. *J. Am. Chem. Soc.* **1998**, *120*, 5279.
- (39) In a benchmark study conducted on 13 isogyric reactions of several small molecules (ref 56), a standard deviation of ~2 kcal/mol for reaction enthalpies [calculated at the CCSD(T)/cc-pCVTZ level] with respect to experimental values was found. However, in these reactions, only the number of electron pairs is conserved, while the number of bonds of a certain type is changed (nonisodesmic reactions). For reactions that are both isogyric and isodesmic, a smaller error in the calculated reaction enthalpy can be expected.
- (40) Rittby, M.; Bartlett, R. J. *J. Phys. Chem.* **1988**, *92*, 3033.
- (41) Stanton, J. F. *J. Chem. Phys.* **1994**, *101*, 371.
- (42) Chiles, R. A.; Dykstra, C. E. *J. Chem. Phys.* **1981**, *74*, 4544.
- (43) Becke, A. D. *J. Chem. Phys.* **1993**, *98*, 5648.
- (44) Raghavachari, K.; Trucks, G. W.; Pople, J. A.; Head-Gordon, M. *Chem. Phys. Lett.* **1989**, *157*, 479.
- (45) Watts, J. D.; Gauss, J.; Bartlett, R. J. *J. Chem. Phys.* **1993**, *98*, 8718.
- (46) Krishnan, R.; Binkley, J. S.; Seeger, R.; Pople, J. A. *J. Chem. Phys.* **1980**, *72*, 650.
- (47) McLean, A. D.; Chandler, G. S. *J. Chem. Phys.* **1980**, *72*, 5639.
- (48) Dunning, T. H. *J. Chem. Phys.* **1989**, *90*, 1007.
- (49) Gauss, J.; Stanton, J. F. *J. Phys. Chem. A* **2000**, *104*, 2865.
- (50) Handy, J. C.; Pople, J. A.; Head-Gordon, M.; Raghavachari, K.; Trucks, G. W. *Chem. Phys. Lett.* **1989**, *164*, 185.
- (51) Kong, J.; White, C. A.; Krylov, A. I.; Sherrill, C. D.; Adamson, R. D.; Furlani, T. R.; Lee, M. S.; Lee, A. M.; Gwaltney, S. R.; Adams, T. R.; Ochsenfeld, C.; Gilbert, A. T. B.; Kedziora, G. S.; Rassolov, V. A.; Maurice, D. R.; Nair, N.; Shao, Y.; Besley, N. A.; Maslen, P.; Dombroski, J. P.; Daschel, H.; Zhang, W.; Korambath, P. P.; Baker, J.; Bird, E. F. C.; Van Voorhis, T.; Oumi, M.; Hirata, S.; Hsu, C.-P.; Ishikawa, N.; Florian, J.; Warshel, A.; Johnson, B. G.; Gill, P. M. W.; Head-Gordon, M.; Pople, J. A. *J. Comput. Chem.* **2000**, *21*, 1532.
- (52) Stanton, J. F.; Gauss, J.; Watts, J. D.; Lauderdale, W. J.; Bartlett, R. J. *ACES II*, 1993. The package also contains modified versions of the MOLECULE Gaussian integral program of J. Almlöf and P. R. Taylor; the ABACUS integral derivative program written by T. U. Helgaker, H. J. Aa. Jensen, P. Jørgensen, and R. Taylor, and the PROPS property evaluation integral code of P. R. Taylor.
- (53) Basis sets were obtained from the Extensible Computational Chemistry Environment Basis Set Database, Version, as developed and distributed by the Molecular Science Computing Facility, Environmental and Molecular Sciences Laboratory, which is part of the Pacific Northwest Laboratory, P.O. Box 999, Richland, WA 99352, and funded by the U.S. Department of Energy. The Pacific Northwest Laboratory is a multi-program laboratory operated by Battelle Memorial Institute for the U.S. Department of Energy under contract DE-AC06-76RLO 1830. Contact David Feller or Karen Schuchardt for further information.
- (54) Krylov, A. I. *J. Chem. Phys.* **2000**, *113*, 6052.
- (55) Szalay, P. G.; Gauss, J. *J. Chem. Phys.* **2000**, *112*, 4027.
- (56) Helgaker, T.; Jørgensen, P.; Olsen, J. *Molecular Electronic Structure Theory*; John Wiley & Sons: New York, 2000.
- (57) Wenthold, P. G.; Hu, J.; Squires, R. R. *J. Am. Chem. Soc.* **1996**, *118*, 11865.
- (58) Ervin, K. M.; DeTuri, V. F. *J. Phys. Chem. A* **2002**, *106*, 9947.